# Archetypal oscillator for smooth and discontinuous dynamics

Qingjie Cao,[1] Marian Wiercigroch,[1,*] Ekaterina E. Pavlovskaia,[1] Celso Grebogi,[1] and J. Michael T. Thompson[1,2]
[1]*Centre for Applied Dynamics Research, Department of Engineering, University of Aberdeen, King's College, Aberdeen AB24 3UE, Scotland, United Kingdom*
[2]*Department of Applied Mathematics and Theoretical Physics, University of Cambridge, Cambridge, CB3 0WA, United Kingdom*
(Received 9 June 2006; revised manuscript received 15 September 2006; published 30 October 2006)

We propose an archetypal system to investigate transitions from smooth to discontinuous dynamics. In the smooth regime, the system bears significant similarities to the Duffing oscillator, exhibiting the standard dynamics governed by the hyperbolic structure associated with the stationary state of the double well. At the discontinuous limit, however, there is a substantial departure in the dynamics from the standard one. In particular, the velocity flow suffers a jump in crossing from one well to another, caused by the loss of local hyperbolicity due to the collapse of the stable and unstable manifolds of the stationary state. In the presence of damping and external excitation, the system has coexisting attractors and also a chaotic saddle which becomes a chaotic attractor when a smoothness parameter drops to zero. This attractor can bifurcate to a high-period periodic attractor or a chaotic sea with islands of quasiperiodic attractors depending on the strength of damping.

DOI: 10.1103/PhysRevE.74.046218 PACS number(s): 05.45.−a, 05.10.−a

## I. INTRODUCTION

This study is motivated by a growing recent interest in nonsmooth dynamics where various physical systems have been studied. Examples include problems from mechanical and civil engineering [1,2], electronics [3,4], control [5,6], computer graphics [7–9], biology [10,11], and others. Although some theoretical foundations have been laid in the work by Filippov [12], Feigin [13], Kunze [14], Peterka [15], Shaw and Holmes [16], and Nordmark [17], there is a large disparity between development and understanding of smooth and discontinuous (nonsmooth) systems.

An archetypal oscillator whose nonlinearity can be smooth or discontinuous depending on the value of the smoothness parameter $\alpha$ is proposed and studied. As the considered oscillator has properties of both a smooth and a discontinuous system (at the limit), potentially a wealth of knowledge can be drawn from the well-developed theory of continuous dynamics. Physically [as shown in Fig. 1(a)] this oscillator is similar to a snapthrough truss system. It comprises a mass $m$ linked by a pair of inclined elastic springs which are capable of resisting both tension and compression; each spring of stiffness $k$ is pinned to a rigid support. This model is inspired by the elastic arch described by Thompson and Hunt in [18] [see Fig. 1(b)]. Although the springs themselves provide linear restoring resistance, the resulting vertical force on the mass is strongly nonlinear because of changes to the geometric configuration.

The equation of motion can be written as

$$m\ddot{X} + 2kX\left(1 - \frac{L}{\sqrt{X^2 + l^2}}\right) = 0, \tag{1}$$

where $L$ is the equilibrium length, $X$ is the mass displacement and $l$ is the half distance between the rigid supports.

Now suppose system (1) is perturbed by a viscous damping and an external harmonic excitation of amplitude $F_0$ and frequency $\Omega$. This leads to the following system:

$$m\ddot{X} + \delta\dot{X} + 2kX\left(1 - \frac{L}{\sqrt{X^2 + l^2}}\right) = F_0 \cos \Omega t. \tag{2}$$

System (1) can be made dimensionless by letting $\omega_0^2 = 2k/m$, $x = X/L$, and $\alpha = l/L \geq 0$,

$$\ddot{x} + \omega_0^2 x\left(1 - \frac{1}{\sqrt{x^2 + \alpha^2}}\right) = 0. \tag{3}$$

The smoothness parameter $\alpha$ not only defines the geometry of the oscillator [Fig. 1(a)] but also has physical meaning. For $\alpha > 1$ the system represents a pretensioned discrete elastic string, while if $\alpha = 0$, the model corresponds to an oscillating mass supported by two parallel vertical springs.

Again the system (2) can be written in a dimensionless form by letting $\tau = \omega_0 t$, $f_0 = F_0/2kL$, $\xi = \delta/2m\omega_0$, and $\omega = \Omega/\omega_0$,

$$x'' + 2\xi x' + x\left(1 - \frac{1}{\sqrt{x^2 + \alpha^2}}\right) = f_0 \cos \omega\tau, \tag{4}$$

where the prime denotes differentiation with respect to $\tau$.

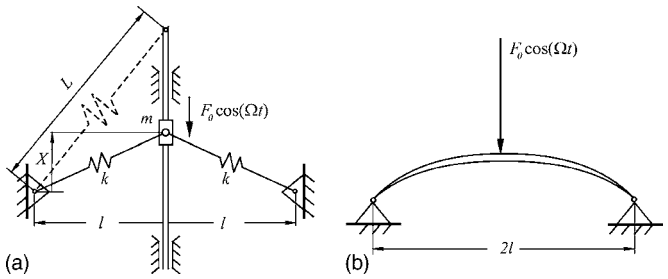


FIG. 1. (a) The dynamical model in the form of a nonlinear oscillator, where a mass is supported by a pair of springs pinned to rigid supports and (b) a simple elastic arch.

*Corresponding author. Electronic address: m.wiercigroch@abdn.ac.uk

 

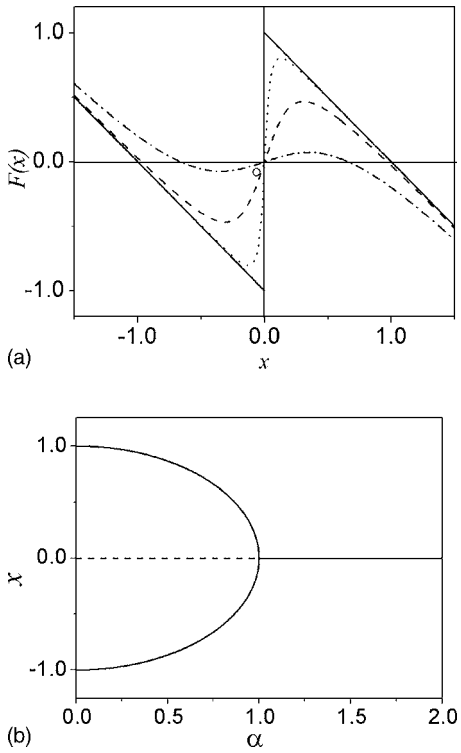


FIG. 2. (a) Nonlinear restoring force $F(x)$; solid line marks the discontinuous case for $\alpha=0$; dotted, dash-dotted, and dashed curves are the smooth cases for $\alpha=0.1$, 0.5, and 0.75, respectively. (b) Bifurcation diagram of system (3).

The nonlinear restoring force $F(x)=-\omega_0^2 x(1-1/\sqrt{x^2+\alpha^2})$ is plotted for $\omega_0=1$ in Fig. 2(a) for different values of parameter $\alpha$. The solid line represents the discontinuous case $\alpha=0$, the dotted, the dash-dotted, and the dashed lines mark the smooth cases, for $\alpha=0.01$, 0.5, and 0.75, respectively.

## II. DISCONTINUOUS UNPERTURBED CASE

When $\alpha=0$ system (3) can be written in the following form:

$$\ddot{x}+\omega_0^2[x-\mathrm{sgn}(x)]=0. \tag{5}$$

It is worth reiterating here that the discontinuous dynamics is obtained by decreasing the smoothness parameter $\alpha$ to 0.

To examine the influence of parameter $\alpha$ on the dynamics of (3) we construct the bifurcation diagram, depicted in Fig. 2(b). The system undergoes a supercritical pitchfork bifurcation at $\alpha=1$ where the stable branch $x=0$ bifurcates into two stable branches at $x=\pm\sqrt{1-\alpha^2}$. The stationary $x=0$ state is now unstable, exhibiting the standard hyperbolic structure. The Hamiltonian for system (3) can be written as

$$H(x,y)=\frac{1}{2}y^2+\frac{1}{2}\omega_0^2x^2-\omega_0^2\sqrt{x^2+\alpha^2}+\omega_0^2\alpha, \tag{6}$$

where $\dot{x}=y$. With the help of the Hamiltonian function (6), the trajectories can be classified and analyzed. For both continuous and discontinuous cases, the phase portraits of systems (3) and (5) are plotted for different values of the Hamiltonian $H(x,y)=E$. For instance, for the smooth nonlinearity, $\alpha=0.5$, the dynamic behavior of the double well is similar to that of the Duffing oscillator [19], shown in Fig. 3(a). For $\alpha=0$, the behavior is singular, as shown in Fig. 3(b): the orbits for $E>0$ are comprised of two large segments of circles with their centers located at $(-1,0)$ and $(1,0)$ connected at $x=0$. The case of $E<0$ is represented by two families of circles.

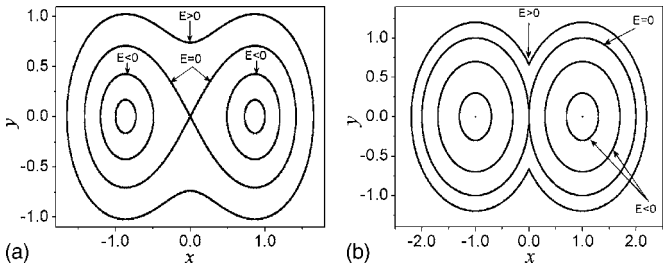


FIG. 3. Phase portraits: (a) smooth case for $\alpha=0.5$ and (b) discontinuous case for $\alpha=0$.

It is most interesting that the orbit of the discontinuous system (5) for $E=0$ is made up of two circles centered at $(\pm1,0)$ connecting at the singular point $(0,0)$, which form special singular homocliniclike orbits. The structure around the point indicates a saddlelike behavior. The hyperbolicity at origin $(0,0)$ is lost due to the tangency of the stable and unstable eigendirections. This isolated singularity has neither eigenvalue nor eigenvector. The pair of circles excluding the point $(0,0)$ are not the manifolds of the singularity, but the flow along these circles approaches the point as $x\to0$, and it will be trapped by the singularity. The solution of the special homoclinic like orbits can be formulated as

$$\Gamma=\left\{(x_\pm(t),y_\pm(t)),t\in\left(-\frac{\pi}{\omega_0},\frac{\pi}{\omega_0}\right)\right\}\cup\{(0,0)\}, \tag{7}$$

where $(x_\pm(t),y_\pm(t))=(\pm1\pm\cos\omega_0 t,\mp\sin\omega_0 t)$.

## III. TRANSITION FROM SMOOTH TO DISCONTINUOUS DYNAMICS

Numerical simulations have been carried out for system (4), assuming $f_0=0.8$, $\xi=0.01\sqrt{2}$, and $\omega=0.75\sqrt{2}$. Figure 4 shows bifurcation diagrams constructed for $x$ sampled stroboscopically at phase zero versus control parameter $\alpha$ as $\alpha$ decreases from 1 to 0 [Fig. 4(a)] and $\alpha$ increases from 0 to 0.3 and from 0.5 to 1 and decreases from 0.5 to 0.3 [Fig. 4(b)]. The system has coexisting periodic attractors and a strange chaotic attractor for $\alpha>0$. However, for $\alpha=0$ the system exhibits chaotic and periodic solutions with unusually high periods. These behaviors can be controlled by the strength of the damping. The main feature of these attractors is their topological similarity since they are associated with the hyperbolic stationary state. This similarity also holds for $\alpha>0$. The chaotic attractor can become a chaotic sea with islands representing quasiperiodic behavior for $\alpha=0$ and $\xi=0$.

Figure 4(a) also shows the coexisting periodic solution of periods 1, 3, 5, and 7 at $\alpha=1$ [orbits are shown in Fig. 5(a)]

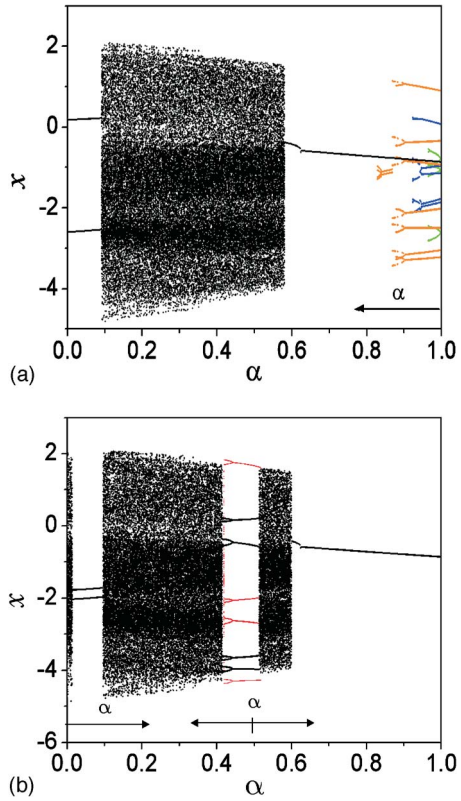


FIG. 4. (Color online) Bifurcation diagrams for $x$ versus $\alpha$ constructed. (a) Decreasing from $\alpha=1$ and following the attractors starting with period 1 (black), 3 (green), 5 (blue), and 7 (red) respectively. (b) First increasing from $\alpha=0$ to 0.3 following the attractor starting with the initial condition (1,0). Second, decreasing $\alpha$ from 0.5 to 0.3 and increasing $\alpha$ from 0.5 to 1, following the attractors starting with two period-4 solutions, respectively.

and their bifurcations under decreasing $\alpha$. Other coexisting periodic solutions are found for $\alpha \in (0,0.1)$, as shown in Figs. 4(a) and 4(b). These two coexisting period-2 solutions are symmetrical and the orbits for $\alpha=0.05$ are presented in Fig. 5(b). For $\alpha \in (0.41,0.52)$ a chaotic attractor coexists with two period-4 solutions and the corresponding trajectories and the chaotic attractor are shown in Figs. 5(c) and 5(d), respectively.

In addition to the coexistence of different attractors, the system exhibits chaotic transients throughout. This behavior can be characterized by chaotic saddles; see [20–22]. The transient and the final periodic attractor are shown in Figs. 6(b) and 6(c) for $\alpha=0.01$ and 0.001, respectively. The set of Poincaré maps shown in Fig. 6 for $\alpha=0.1,0.01,0.001$, and 0 shows the topological similarity now associated with the discontinuity at the origin. The coexisting period-2 solutions persist for $\alpha=0$ and the chaotic saddle becomes a chaotic attractor for $\alpha=0$ as shown in Fig. 6(d). The behavior of this chaotic attractor can be controlled by the damping ratio $\xi$. Other attractors are presented in Fig. 7(a) for $\xi=0.005$, Fig. 7(b) for $\xi=0.0125$, and Fig. 7(c) for $\xi=0.025$. A high-period periodic attractor is shown in Fig. 7(d) having period 23 for $\xi=0.028$. For both $\alpha=0$ and $\xi=0$, a chaotic sea and quasi-periodic behavior can also be inferred via a semi-analytical method, see [23]. Figure 8 shows the chaotic sea together

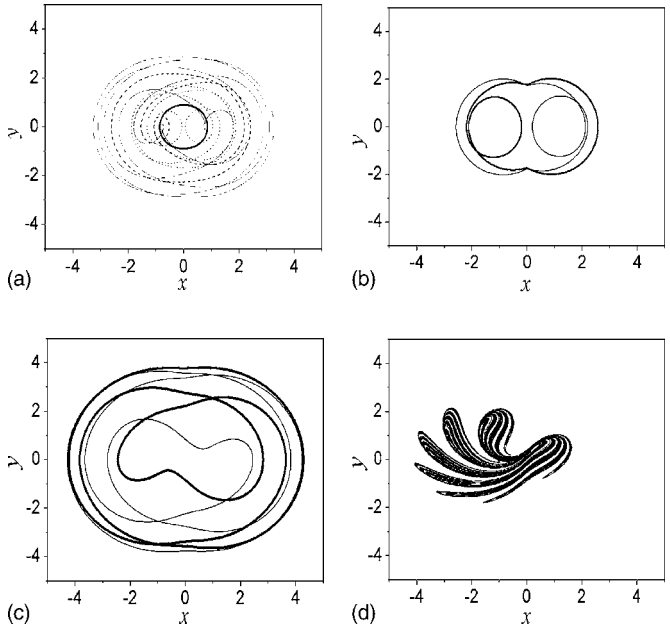


FIG. 5. Coexistence of periodic motions. (a) Period 1 (thick line), 3 (dashed line), 5 (dotted line), and 7 (thin line), respectively, for $\alpha=1.0$. (b) A pair of period-2 solutions for $\alpha=0.05$. (c) and (d) represent the pair of period 4 and the chaotic attractor for $\alpha=0.5$ with the largest Lyapunov exponent 0.1065.

with a pair of quasi-period-2 solutions, a pair of quasi-period-5 solutions, the quasi-period-9 and the quasi-period-11 solutions, respectively.

The largest Lyapunov exponents for all the chaotic attractors presented in this paper have been calculated using the chaos synchronization method (see [24] for instance), as shown in the captions for the corresponding figures.

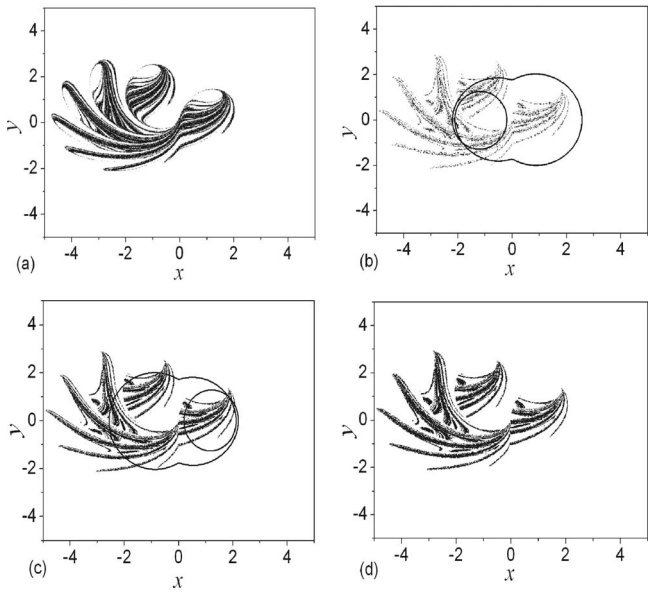


FIG. 6. (a) Chaotic attractor for $\alpha=0.1$ with the largest Lyapunov exponent 0.0812. (b) Chaotic saddle leading to period-2 solution for $\alpha=0.01$. (c) Chaotic saddle leading to period-2 solution for $\alpha=0.001$. (d) Chaos for $\alpha=0$ with the largest Lyapunov exponent 0.0480.

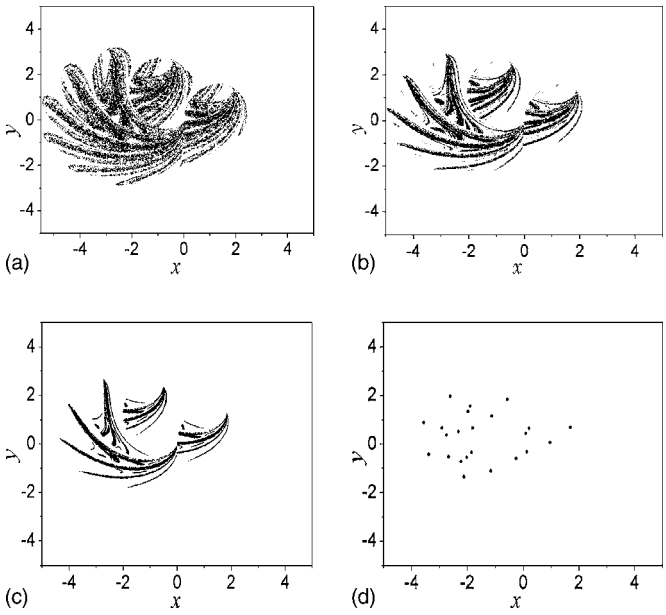


FIG. 7. Poincaré sections for $f_0=0.8$, $\omega=0.75\sqrt{2}$, $\alpha=0$. (a) Chaotic attractor for $\xi=0.005$ with the largest Lyapunov exponent 0.0525. (b) Chaotic motion for $\xi=0.0125$ with the largest Lyapunov exponent 0.0505. (c) Chaotic motion for $\xi=0.025$ with the largest Lyapunov exponent 0.0470. (d) High-periodic motion of period 23 for $\xi=0.028$.

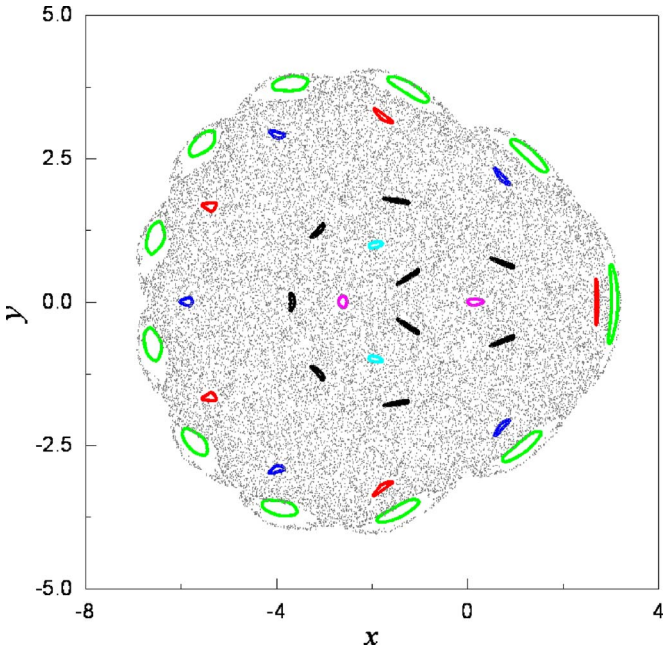


FIG. 8. (Color online) Poincaré section for $f_0=0.8$, $\omega=0.75\sqrt{2}$, $\alpha=0$: Chaotic sea and quasiperiodic trajectories (islands) for $\xi=0$.

## IV. CLOSING REMARKS

A smooth or discontinuous nonlinear oscillator has been proposed. The nonlinearity can be smooth or discontinuous depending on the value of the smoothness parameter $\alpha$. A mathematical model of the oscillator has been developed and investigated. It has been found that the unperturbed smooth system has a double-well characteristic which is similar to the Duffing oscillator. The discontinuous system exhibits a saddlelike singularity connecting two circles forming homocliniclike orbits. Under perturbation, for large $\alpha$, the system exhibits complex coexistence of periodic attractors and also periodic solutions with a strange chaotic attractor which disappears at $\alpha\approx 0.1$. Decreasing $\alpha$ further creates chaotic transients around a chaotic saddle, which leads to periodic orbits as time increases. This chaotic transient becomes a chaotic attractor for $\alpha=0$. The attractor can deform in shape or bifurcate to a high-period periodic attractor depending on the strength of damping, or can even become a chaotic sea with islands of quasiperiodic trajectories for $\xi=0$. It is also interesting to compare the fingerlike topology of the chaotic attractors found in this paper with that observed by Thompson *et al.* in [25,26]. The latter arose in a linear oscillator with impacts, which has apparent similarities with the present model.

The presented oscillator is being actively studied by the authors in two main directions. First, the peculiar properties at the limit of $\alpha=0$ are being analyzed in more detail to better understand the bifurcation structures under varying damping and external forcing. This research relates to the studies of preloaded oscillators, e.g., [2,27]. The second pursued direction is to develop analytical measures (e.g., construction of the Melnikovian) to predict the border of chaos. This research bears a significant analogy to the predictions made for the Duffing oscillator; see, e.g., [28,29].

## ACKNOWLEDGMENTS

Q.C. acknowledges financial support from EPSRC under Grant No. GR/R85556, and from the Scottish Enterprise.

[1] E. E. Pavlovskaia, M. Wiercigroch, K.-C. Woo, and A. A. Rodger, Meccanica **38**, 85 (2003).
[2] E. Pavlovskaia, E. V. Karpenko, and M. Wiercigroch, J. Sound Vib. **276**, 361 (2004).
[3] S. Banerjee and K. Chakrabarty, IEEE Trans. Power Electron. **13**, 252 (1998).
[4] S. Banerjee, E. Ott, J. A. Yorke, and G. H. Yuan, *Proceedings of the Power Electronics Specialists' Conference*, 1997 (unpublished), pp. 1337–1344.
[5] J. J. Slotine and S. S. Sastry, Int. J. Control **38**, 465 (1983).
[6] P. Y. Richard, H. Cormerais, and J. Buisson, Nonlinear Anal. Theory, Methods Appl. **65**, 1751 (2006).
[7] A. Luo and H. Burkhardt, Int. J. Comput. Vis. **15**, 171 (1995).
[8] Tomoyuki Nishita, Thomas W. Sederberg, and Masanori Kakimoto, Comput. Graphics **24**, 337 (1990).
[9] X. Gu, Y. He, and H. Qin, Graphical Models **68**, 237 (2006).
[10] C. M. Kribs-Zaleta, Math. Biosci. **192**, 137 (2004).
[11] S. Drulhe, G. Ferrari-Trecate, H. De Jong, and A. Viari, Lect.

Notes Comput. Sci. **3927**, 184 (2006).
[12] A. F. Filippov, *Differential Equations with Discontinuous Right-Hand Sides* (Kluwer Academic Publishers, Dordrech, 1988).
[13] M. I. Feigin, *Forced Vibrations of Nonlinear Systems with Discontinuities* (Nauka, Moscow, 1994) (in Russian).
[14] M. Kunze, *Non-Smooth Dynamical Systems* (Springer-Verlag, Berlin, 2000).
[15] F. Peterka, *Introduction to Vibration of Mechanical Systems with Internal Impacts* (Academia Publishing House, Prague, 1981) (in Czech).
[16] S. W. Shaw and P. J. Holmes, J. Sound Vib. **90**, 129 (1983).
[17] A. B. Nordmark, J. Sound Vib. **145**, 279 (1991).
[18] J. M. T. Thompson and G. W. Hunt, *A General Theory of Elastic Stability* (John Wiley & Sons, London, 1973).
[19] J. Guckenheimer and P. Holmes, *Nonlinear Oscillation, Dynamical System and Bifurcation of Vector Fields* (Springer-Verlag, New York, 1983).
[20] Y. C. Lai and R. L. Winslow, Phys. Rev. Lett. **74**, 5208 (1995).
[21] T. Tel, Phys. Lett. A **119**, 65 (1986).
[22] C. Grebogi, E. Ott, and J. A. Yorke, Physica D **7**, 181 (1983).
[23] E. Pavlovskaia and M. Wiercigroch, Chaos, Solitons Fractals **19**, 151 (2004).
[24] A. Stefanski and T. Kapitaniak, Chaos, Solitons Fractals **15**, 233 (2003).
[25] J. M. T. Thompson and R. Ghaffari, Phys. Rev. A **27**, 1741 (1983).
[26] J. M. T. Thompson and H. B. Stewart, *Nonlinear Dynamics and Chaos*, 2nd ed. (Wiley, Chichester, 2002).
[27] F. Peterka, Chaos, Solitons Fractals **18**, 79 (2003).
[28] Y. Ueda, S. Yoshida, H. B. Stewart, and J. M. T. Thompson, Philos. Trans. R. Soc. London, Ser. A **332**, 169 (1990).
[29] A. N. Lansbury, J. M. T. Thompson, and H. B. Stewart, Int. J. Bifurcation Chaos Appl. Sci. Eng. **2**, 505 (1992).